Gravity field inversion using Improved Particle Swarm Optimization (IPSO) for estimation of sedimentary basin basement depth

Soudeh LONI ⓘD, Mahmoud MEHRAMUZ* ⓘD

Department of Earth Sciences, Science and Research Branch, Islamic Azad University, Tehran, Iran

Abstract: In this paper, for the first time an Improved Particle Swarm Optimization (IPSO) algorithm, is developed to evaluate the 2.5-D basement of sedimentary basin and consequently to simulate its bottom, by using the density contrast that varies parabolically with depth simultaneously. The IPSO method is capable of improving the global search of particles in all of the search fields. Finding the optimum solution is adjusted by an inertia weight and acceleration coefficients. Here, we have examined the ability of the IPSO inversion by the synthetic gravity data due to a sedimentary basin, with and without noise. The calculated depth and gravity of the synthetic model do not differ too much from assumed values due to set limits for model parameters and are always within the range. Also, the mentioned method has been applied for the 2.5-D gravity inverse modelling of a sedimentary basin in Iran. We also have modelled the sedimentary basin in 2-D along seven profiles. Furthermore, using the depth values estimated by IPSO from all profiles, a 3-D model of the sedimentary basin was generated. The obtained maximum depth for this sedimentary basin is 2.62 km.

Key words: IPSO, inverse modelling, gravity data, sedimentary basin

1. Introduction

The sedimentary basin is one of the geological structures for the investigation of hydrocarbon traps. For this aim, the gravity inversion is used to estimate the depth of sedimentary basin. Several authors have proposed various optimization approaches for the 2-D and 2.5-D sedimentary basin to analyse gravity anomalies while the density of sediments is considered constant (*Gadirov et al., 2016; Annecchione et al., 2001; Barbosa et al., 1999; Rao et al., 1994; Litinsky, 1989; Murthy and Rao, 1989; Murthy et al.,1988;*

---

*corresponding author: e-mail: m.mehramooz@srbiau.ac.ir

Won and Bavis, 1987; Bhattacharya and Navolio, 1975). *Chakravarthi and Sundararajan (2005 and 2007)* applied the parabolic density contrast to simulate 2.5-D sedimentary basin. *Chakravarthi and Ramamma (2015)* utilized exponential density function to compute a sedimentary basin basement depth. *Karcol (2018)* generalized the solution for the gravitational potential and its derivatives of the right rectangular prism with depth-dependent density that can be approximated by an n-th degree polynomial. Further, many linear inverse modelling methods have been developed to simulate the sedimentary basin basement (*Sun and Li, 2014; Gallardo-Delgado et al., 2003*).

Particle Swarm Optimization (PSO) is a relatively recent method and one of the most popular nature-inspired heuristic optimization algorithm created by *Kennedy and Eberhart (1995)*. PSO has been successfully employed in some fields of geophysics: such as reversal of self-potential of idealized bodies' anomalies (*Monteiro Santos, 2010*), gravity assessment of a fault and estimation of its parameters such as angle of the fault, thickness of the sheet, and left and right distances to the middle of the sheet using PSO (*Toushmalani, 2013a and b*), the application of the members of PSO family to the 2-D and 3-D gravity inversion and uncertainty assessment of basement relief in sedimentary basins (*Pallero et al., 2015 and 2017*), focus on the use of a PSO algorithm to sample the region of equivalence in non-linear inverse problems (*Pallero et al., 2018*), the use of PSO for the inversion of gravity in 2.5-D sedimentary basins (*Singh and Singh, 2017*), inversion of residual gravity anomalies utilizing tuned PSO (*Roshan and Singh, 2017*), interpretation of gravity data using PSO (*Essa and Elhussein, 2018a*), utilizing a robust PSO to evaluate magnetic data of 2-D dipping dike (*Essa and Elhussein, 2017*), and use of the PSO to interpret magnetic anomalies due to simple geometrical bodies (*Essa and Elhussein, 2018b*).

The advantages of PSO are relative simplicity and easy implementation. However, the algorithm disadvantages can be premature convergence and possible falling into a local minimum. In this paper, for the first time, we have suggested an IPSO algorithm with an improved inertia weight coefficient (w) and learning factors (c_1,c_2) to solve this problem and used it to estimate the depth of sediments based on the gravity data, by using the density contrast that changes parabolically with depth.

2. Method

2.1. Gravity anomaly of a sedimentary basin

Fig. 1 demonstrates the geometrical form of the 2.5-D rectangular prism that its strike length, width and a minimum distance between the centre of each prism to the profile, RR*, their values are $2S$, $2b$, s, respectively. Several juxtaposed 2.5-D rectangular prisms can be used to simulate the sedimentary basin.

A gravity anomaly can be obtained at each point of observation, $P(x_k, 0)$, that cover the sedimentary basin (*Chakravarthi and Sundarajan, 2006*) as:

$$g_b = \sum_{y=2}^{N-1} g_i(x_k, 0),\tag{1}$$

where N is the number of gravity measurement points on the profile, RR*, and $g_i(x_k, 0)$ is the gravity anomaly of the i-th prism at any point that was introduced by *Chakravarthi and Sundararajan (2005)* as:

$$g(x_k, 0) = \int_{w=d_1}^{d_2} \int_{v=-S}^{S} \int_{u=-b}^{b} \frac{G\,\Delta\rho(w)\,w\,\mathrm{d}u\mathrm{d}v\mathrm{d}w}{[(y-x_k)^2 + v^2 + w^2]^{3/2}},\tag{2}$$
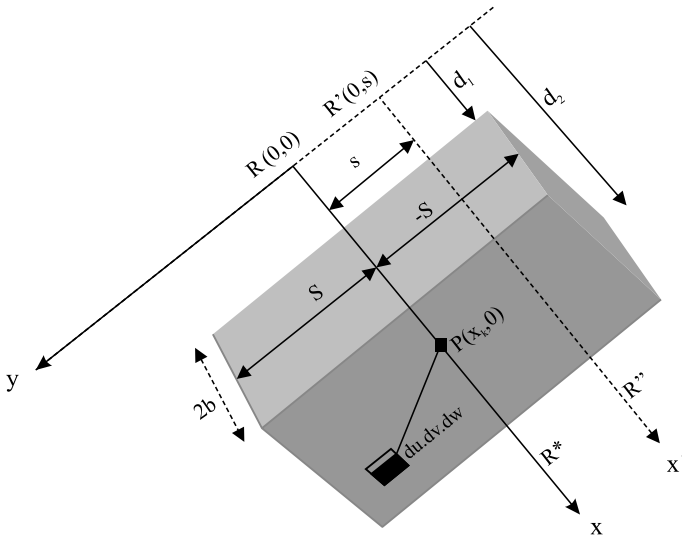

Fig. 1. A 2.5-D rectangular prism that its strike length, width and offset distance of profile, RR*, is $2S$, $2b$, s.

where G is the universal gravitational constant and $\mathrm{d}u\mathrm{d}v\mathrm{d}w$ is a volume element of prism, d_1 and d_2 are upper and lower depth of the prism, respectively. $\Delta\rho(w)$ is the parabolic density contrast that was developed by *Chakravarthi et al. (2001)* as:

$$\Delta\rho(w) = \frac{\Delta\rho_0{}^3}{(\Delta\rho_0 - \alpha w)^2}, \tag{3}$$

$\Delta\rho_0$ is the density contrast evaluated at the ground surface and α is the rate of variation of density contrast expressed in length units. $\Delta\rho_0$ and α can be determined by fitting the field data of density contrast vs. depth in the least square sense to Eq. (3) (*Rao et al., 1995*). Substituting Eq. (3) in Eq. (2), the calculated gravity is obtained as:

$$
\begin{aligned}
g(x_k, 0) = -2G\Delta\rho_0{}^3 \Bigg\{ \Bigg\langle & \frac{\alpha x_k S}{t_4}\left(\frac{1}{t_4} + \frac{1}{t_3}\right)\ln\frac{t_5}{t_6} + \frac{S}{2t_2}\ln\frac{(R + x_k)}{(R - x_k)} + \\
& + \frac{x_k}{2t_3}\ln\frac{(R + S)}{(R - S)} + \frac{\Delta\rho_0}{\alpha}\left[\frac{1}{t_2}\tan^{-1}\frac{SR}{wX_k} + \frac{1}{t_3}\tan^{-1}\frac{x_k R}{wS}\right] - \\
& - \frac{1}{\alpha t_5}\tan^{-1}\frac{Sx_k}{wR} \Bigg\rangle_{x_k - b}^{x_k + b} \Bigg\}_{d_1}^{d_2}.
\end{aligned} \tag{4}
$$

Here:

$R = x_k{}^2 + S^2 + w^2$,

$t_1 = x_k{}^2 + S^2$,

$t_2 = S^2\alpha^2 + \Delta\rho_0{}^2$,

$t_3 = x_k{}^2\alpha^2 + \Delta\rho_0{}^2$,

$t_4 = \sqrt{t_1\alpha^2 + \Delta\rho_0{}^2}$,

$t_5 = \Delta\rho_0{}^2 - \alpha w$,

$t_6 = -2(\alpha R t_4 + t_1\alpha^2 + \Delta\rho_0\alpha w)$.

2.2. Improved Particle Swarm Optimization (IPSO)

The PSO method simulates the social behaviour of particles, it optimizes their situation based on artificial intelligence. During the assessment procedure, the situation of every particle may vary with every iteration. In the

other words, during the trend of iteration, the particle position is renovated so that the particle finds the best of its position, 'pbest', and the best of its position among the collection of particles, 'gbest'. Consequently, to find the best position, each particle tries to change its current velocity to optimise its position. The velocity of particle is modified to reach a new position utilizing the following equations provided by *Sweilam et al. (2007)* as:

$$V_i^{t+1} = wV_i^t + c_1 \, \mathrm{rand}()(\mathrm{pbest}_i - X_i^t) + c_2 \, \mathrm{rand}()(\mathrm{gbest}_i - X_i^t) \, , \tag{5}$$

$$X_i^{t+1} = X_i^t + V_i^{t+1} \, . \tag{6}$$

V_i^t, X_i^t are current velocity and position of i-th particle at the t-th iteration, rand() function generates random numbers between 0–1, c_1, c_2 are learning factors with constant and positive values that control both the personal and the social behaviour and w is an inertial coefficient with a magnitude generally marginally below 1. The aim of the w is to achieve a balance between exploration and exploitation (global and local search).

Easiness and simplicity of execution are the advantages of the PSO algorithm but falling into the local minimum and premature convergence are its disadvantages. In this paper, we suggest an IPSO algorithm that adjusts inertia weight (w) and learning factors (c_1, c_2) to solve this problem.

In order to avoid premature convergence to local optimality and increase convergence speed, the IPSO algorithm is being used. For this purpose, the inertia weight (w) coefficient and learning factors (c_1, c_2) are improved. The various inertia weighting strategies are categorized into three classes: constant and random inertia weight, time-varying inertia weight, and adaptive inertia weight (*Nickabadi et al., 2011*). In this paper, we use time-varying inertia in order to determine the value of w based on the iteration number. This method can be linear or non-linear and decreasing or increasing. Here, the linearly decreasing technique is used to modify the inertia weight of particle in the following equation (*Xin et al., 2009*):

$$w = \frac{T_{\max} - t_{\mathrm{it}}}{T_{\max}} (w_{\max} - w_{\min}) + w_{\max} \, , \tag{7}$$

where t_{it} and $T_{\max}$ are the number of current and maximum iteration. The value of w decreases from $w_{\max}$ to $w_{\min}$. Based on the results obtained (*Shi and Eberhart, 1998*) the performance of linearly decreasing strategy can be improved significantly when $w_{\max} = 0.9$ and $w_{\min} = 0.4$.

The learning factors (c_1, c_2) are traditionally both equal to 2 (*Sweilam et al., 2007*). However, utilizing recent literature, electing c_1 more predominant than c_2 and $c_1 + c_2 \leq 4$ may lead to the better conclusions (*Parsopoulos and Vrahatis, 2002*). In order to improve the proficiency of PSO, the values of two operators c_1 and c_2 are updated by two dynamic linear equation, respectively, at each iteration (*Yi, 2016*) as follows:

$$c_1 = 2.4 - \frac{1.4\, t_{\text{it}}}{T_{\max}}, \tag{8}$$

$$c_2 = 0.9 + \frac{1.6\, t_{\text{it}}}{T_{\max}}. \tag{9}$$

With this strategy, c_1 can be decreased and c_2 can be increased by increasing the number of iterations. The global investigation capability of particles can be improved by this approach in the whole search space.

When the differences between the observed and calculated gravity data are minimized, the best exact values of the particles (model parameters) are obtained. For this purpose, we use the following simple objective function:

$$Q = \frac{2 \sum_i^N |g_i^o - g_i^c|}{\sum_i^N |g_i^o - g_i^c| + \sum_i^N |g_i^o + g_i^c|}, \tag{10}$$

where N is the number of the gravity measurement points, g_i^o, g_i^c are the observed and calculated gravity anomaly at the point $P(x_i)$, respectively.

The misfit between observed and calculated gravity data is estimated through the average relative error, which is computed by the following equation:

$$ms = \frac{100}{N} \sqrt{\sum_i^N \left(\frac{g_i^o - g_i^c}{g_i^o} \right)^2}. \tag{11}$$

The optimization process repeats until the required number of iterations is completed or the current value of the objective function, Eq. (10), reaches below a predetermined allowable error.

3. Synthetic example

Fig. 2 displays a view from above of a theoretical sedimentary basin structure which has been approximated by a series of rectangular prisms posi-
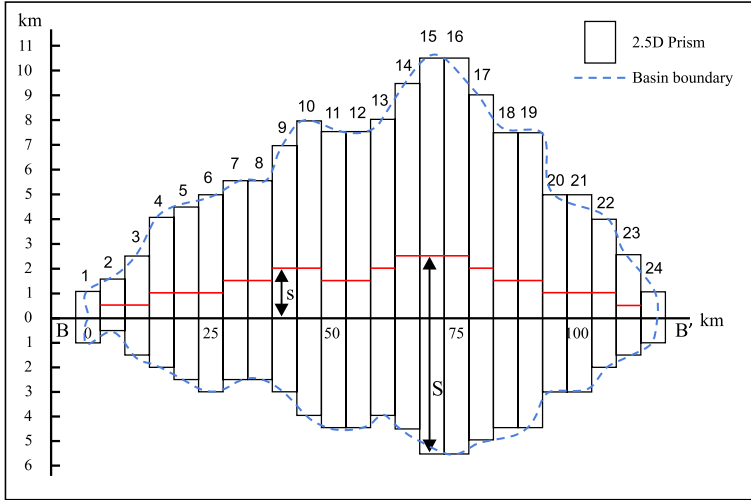
Fig. 2. A sedimentary basin composed of a series of rectangular prisms.

tioned in adjacency and having the same widths as a top of each prism. The characteristics of each prism have been brought in Table 1. The gravity effect of the sedimentary basin is computed at 24 points in the centre of each prism over 115 km profile BB′ with 5 km interval. The values of $\Delta\rho_0$ and α are assumed as -0.65 g/cm^3 and $0.04 \text{ g/cm}^3/\text{km}$, respectively.

Table 1. Specifications of each numbered prism shown in Fig. 2.

Prism	Depth [km]	S [km]	s [km]	Prism	Depth [km]	S [km]	s [km]
1	0	1	0	13	3	6	−2
2	0.5	1	−0.5	14	4	7	−2.5
3	1	2	−0.5	15	5	8	−2.5
4	1	3	−1	16	4.5	8	−2.5
5	1.5	3.5	−1	17	4	7	−2
6	2	4	−1	18	3.5	6	−1.5
7	2.5	4	−1.5	19	4.5	6	−1.5
8	3	4	−1.5	20	3	4	−1
9	3	5	−2	21	2.5	4	−1
10	3.5	6	−2	22	2	3	−1
11	3	6	−1.5	23	1	2	−0.5
12	2.5	6	−1.5	24	0	1	0

According to the defined search ranges for the depth parameter, as shown in Table 2, eighty primary models were randomly constructed. These ranges include the values assumed for the initial model. The number of iterations and predefined error are considered as 90 and 0.002, respectively. The code has performed 90 iterations before the objective function error between the calculated and synthetic gravity falls below the allowable error.

Fig. 3b depicts the assumed depths and estimated ones using IPSO for each prism. The generated gravity anomaly using IPSO inversion has been displayed in Fig. 3a. Fig. 3c shows the error variation versus iteration number. The numerical outputs of the IPSO inversion are listed in Table 2. The estimated misfit by the Eq. (11) at the last iteration is 0.23%.

We assess the effect of error on the ability of the IPSO by adding 5% noise to the gravity response of the sedimentary basin model (Fig. 4a) by the following equation:

$$g_{\text{noise}}(x_i) = g(x_i) + M(\text{rand}(i) - 0.5),\qquad(12)$$

where $g_{\text{noise}}(x_i)$ is the noisy gravity anomaly value at x_i, M controls the noise level (here M is 5) and rand(i) is a pseudo-random number that its range varies between 0 to 1.

The initial presumptions for the synthetic gravity anomalies corrupted with noise are the same as noise-free ones. Besides, for the noise corrupted gravity data, 90 iterations were considered to be completed. Fig. 4b depicts the assumed depths and estimated ones using IPSO for each prism by the contaminated gravity data. The gravity responses corresponding with the inverted depth using IPSO has been displayed in Fig. 4a. Fig. 4c shows the error change versus iteration number. The numerical results of the IPSO inversion for noisy data are given in Table 2. The estimated misfit by the Eq. (11) at the last iteration is 1.307%.

According to IPSO results, the maximum depth error happens for the first and latest prisms, because the gravity anomaly values at these stations are known to be zero. Regardless of these foregoing points, the biggest difference between the assumed and estimated depths, while the data are noise-free and corrupted with noise, are 0.09 km and 0.14 km, respectively. The estimated depths demonstrate the acceptable proficiency of the IPSO inversion method.
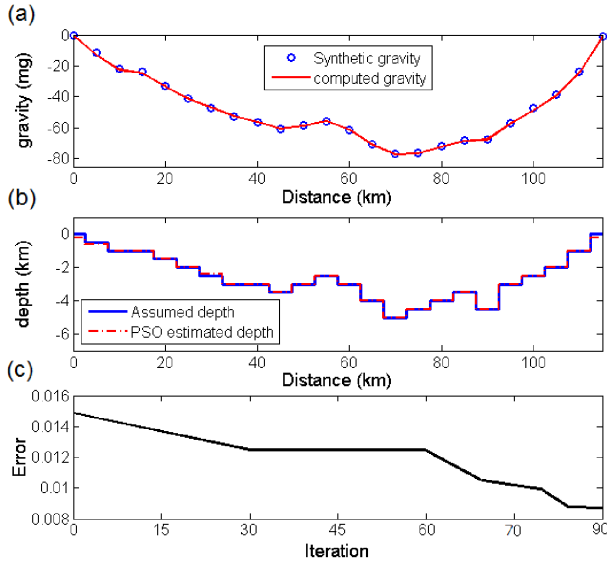
Fig. 3. (a) Synthetic and computed gravity due to (b) assumed and interpreted basement model by IPSO (c) error changes estimated by objective function versus iteration number.
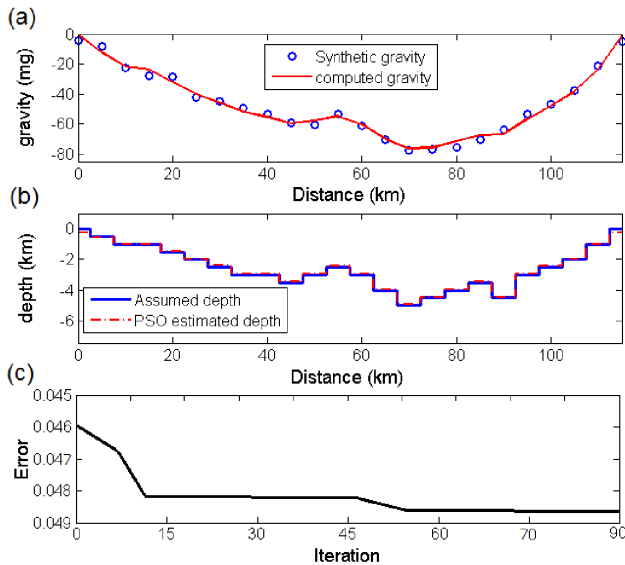

Fig. 4. (a) Synthetic gravity data with 5% added noise and computed gravity due to (b) assumed and interpreted basement model by IPSO (c) error changes estimated by objective function versus iteration number.

311

Table 2. The values of assumed ranges for depths and inverted depths using IPSO, while the data are noise-free and corrupted with noise.

Prism	Assumed range for depth [km]	Estimated depth [km]		Prism	Assumed range for depth [km]	Estimated depth [km]	
		Free	Noisy			Free	Noisy
1	0 − 1	0.18	0.22	13	1.5 − 4.5	3	2.95
2	0 − 1	0.57	0.55	14	2 − 6	4	3.95
3	0.5 − 2	1.06	1	15	3 − 7	5	4.96
4	0.5 − 2	1.06	1	16	2 − 6	4.51	4.45
5	0.5 − 2.5	1.51	1.45	17	2 − 6	4	3.95
6	1 − 3	2	1.95	18	2 − 5	3.51	3.45
7	1.5 − 4	2.41	2.36	19	2 − 6	4.51	4.45
8	1.5 − 4.5	3	2.95	20	1.5 − 4.5	3	2.95
9	1.5 − 4.5	3	2.95	21	1.5 − 4	2.51	2.45
10	2 − 5	3.51	3.45	22	1 − 3	2	1.95
11	1.5 − 4.5	3	2.95	23	0.5 − 2	1.05	1
12	1.5 − 4	2.51	2.45	24	0 − 1	0.21	0.23

4. Field example

The region under investigation is located in Golestan Province, northeastern Iran onto UTM zone 40N, between 367000–412500 m E and 4182000–4198000 m N. This region lies on the Kopet-Dagh basin and structural unit covered by the quaternary thick sediments and rock units of Cretaceous Period. The Fig. 5 shows a geological map of the studied area. The Cretaceous sediments of the Kopet-Dagh basin comprise Shurijeh, Trigan, Sarcheshmeh, Sanganeh, Aitamir, Abderaz, Abtalkh, Neyzar and Kalat formation. This general stratigraphy has been shown in Fig. 6. The Tirgan formation is mainly formed by oolitic and bioclastic limestone with subordinate layers of marl, marine limestone, and calcareous shale. It forms the basement of the sedimentary basin because of its rigidity and erosion resistance.

In order to study the geological structures such as anticline and syncline (that can capture pockets of hydrocarbons in the bend of the arch) and determine the thickness of the sediments, the gravity data sampling was done along 7 profiles with the interval of 1.5 km along profiles A, B, C, E, G and interval of 3 km along profiles D, F by using LaCoste & Romberg gravimeter with an accuracy of 0.01 mGal. The distance between profiles is approximately 2 km. The values of are respectively assumed as $-0.75 \, \text{g/cm}^3$
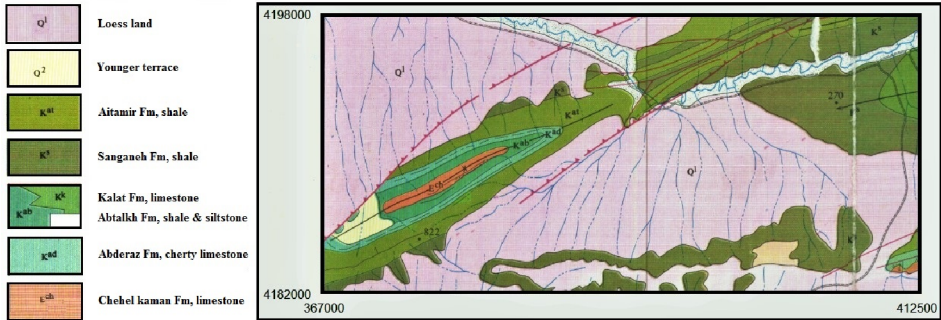
Fig. 5. Geological map of studied area. Scale 1:250000 (Geological survey and mineral exploration of Iran).
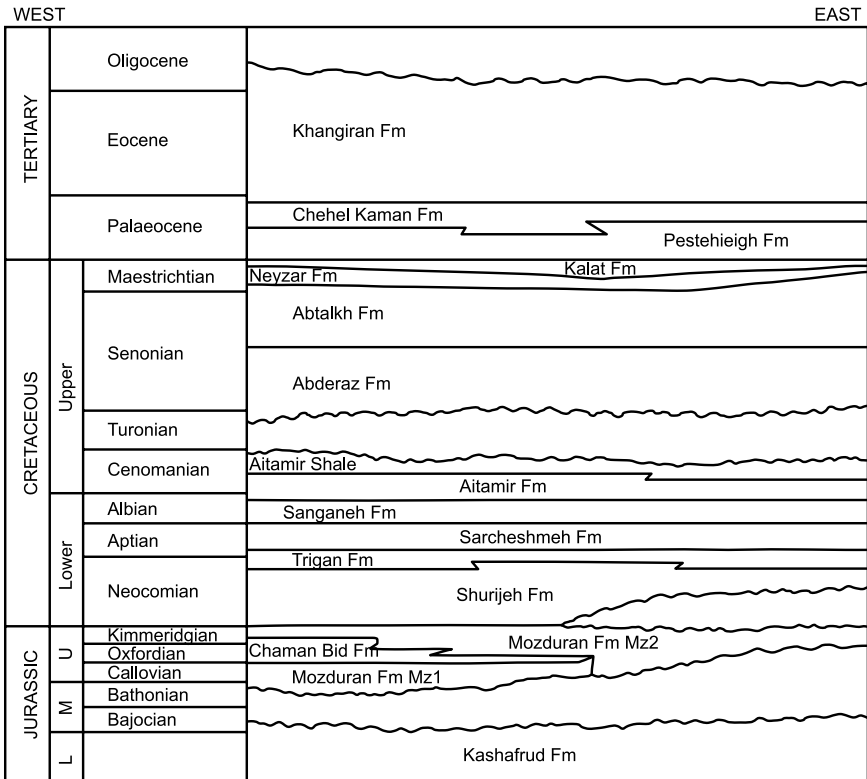

Fig. 6. General stratigraphy of the Kopet-Dagh basin (*Margottini et al., 2013*, page 568).

and $0.08 \text{ g/cm}^3/\text{km}$.

Fig. 7 shows the Bouguer gravity anomaly map of the understudied region. The residual gravity anomaly was obtained by separating the effect of the regional gravity anomaly from the Bouguer gravity anomaly (Fig. 8). The extensive negative anomaly noticeable in the residual gravity map centre is related to a sedimentary basin structure where the 16 prisms simulated the volume of the sedimentary basin (Fig. 8). The considered ranges for the depth of each prism have been given in Table 3. The gravity data sampling
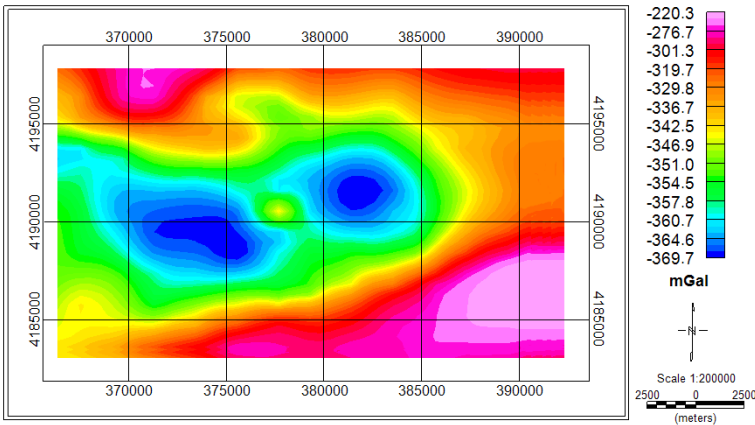
Fig. 7. The Bougure gravity anomaly map of the understudied region.
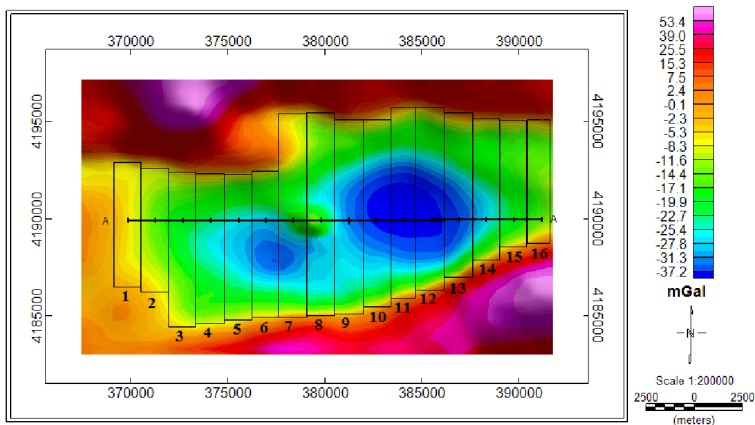
Fig. 8. The residual gravity anomaly map (the position of profile A and prisms have been shown).

was carried out at 16 stations with an interval of 1.5 km along the profile A in the gravity anomaly for inverse modelling using IPSO, as shown in Fig. 9a. The number of iterations and predefined error are considered as 100 and 0.01, respectively. The optimization process is finished before the assigned limit of 100 iterations if the objective function error between the computed and real gravity descends below the assigned error.

Table 3. Depth ranges used in IPSO inversion of the real gravity and obtained results.

Prism	Ranges [km]	Results [km]	Prism	Ranges [km]	Results [km]
1	–	0	9	0.5 − 3	1.37
2	0 − 1	0.17	10	0.7 − 3.5	2.1
3	0.1 − 2	0.44	11	0.7 − 3.5	2.35
4	0.2 − 2	0.64	12	0.5 − 3.5	1.85
5	0.3 − 2.5	0.77	13	0.5 − 3	1.55
6	0.5 − 2.5	1.05	14	0.5 − 2.5	0.95
7	0.3 − 2.5	0.63	15	0.3 − 2.5	0.63
8	0.3 − 2.5	0.74	16	–	0

The gravity response and the depth solutions using IPSO inversion have been demonstrated in Figs. 9a and b. The inverted depths using IPSO have been written in Table 3. Fig. 9c shows the error change versus iteration number. The estimated misfit at the last iteration is 1.314%.

In order to create of a 3-D model of the sedimentary basin basement, in addition, to profile A, another six profiles have been considered, as are shown in Fig. 10. The sampling interval over profiles B, C, E, and G is 1.5 km and for profiles D and F is 3 km. The gravity field variations along these profiles and generated gravity responses corresponding to the inverted depths using IPSO are shown in Figs. 11 to 16. Figs. 11c to 16c show the changes of error estimated by objective function versus the number of iteration for the profiles B, C, D, E, F, and G, respectively. The obtained misfits from the interpretation of the gravity data due to the profiles B, C, D, E, F and G at the last iteration are 1.26, 1.22, 1.88, 1.39, 1.16 and 1.04 percent, respectively.

We have extracted the geographical coordinates corresponding to the each estimated depth value by IPSO. To simulate the basement of sedimentary basin, Oasis Montaj software was applied. Fig. 17 presents the 3-D
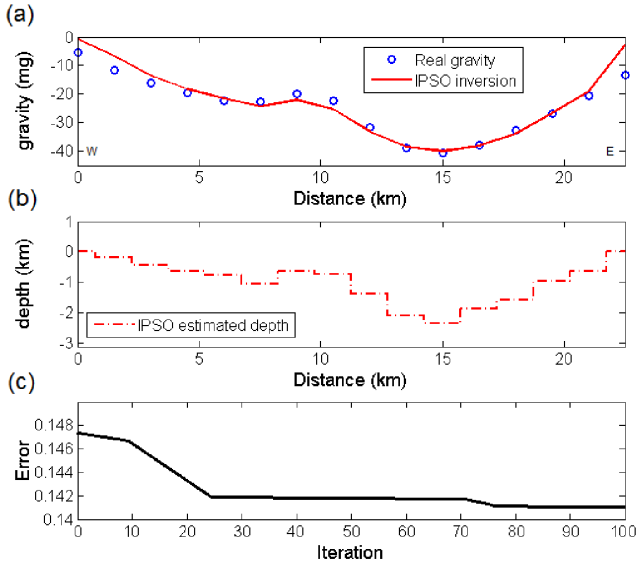
Fig. 9. (a) Real gravity along Profile A and computed gravity (b) interpreted basement model by IPSO (c) error changes estimated by objective function versus iteration number.
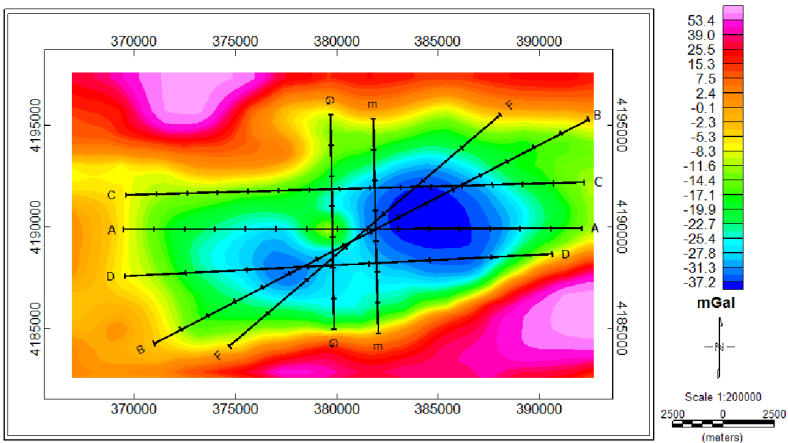

Fig. 10. Location and direction of the profiles A, B, C, D, E, F and G over the residual gravity anomaly map have been specified.

view of the sedimentary basin under study. The maximum depth of the sedimentary basin basement, in other words, maximum sedimentary thickness is 2.62 km.
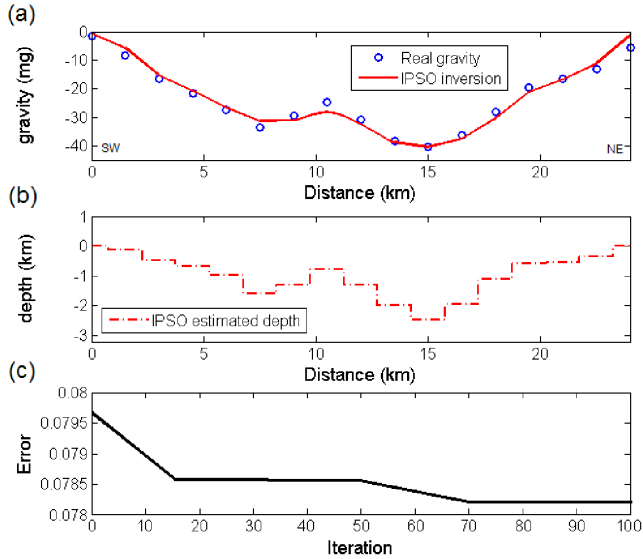
316

Fig. 11. (a) Real gravity along Profile B and computed gravity (b) interpreted basement model by IPSO (c) changes of error estimated by objective function versus the number of iteration.
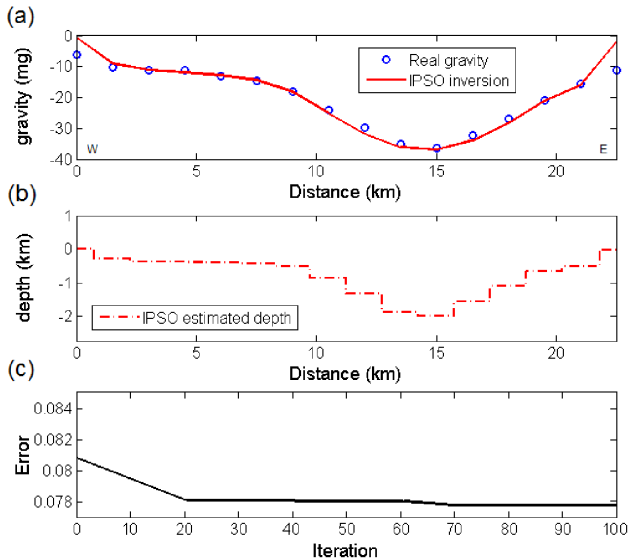

Fig. 12. (a) Real gravity along Profile C and computed gravity (b) interpreted basement model by IPSO (c) changes of error estimated by objective function versus the number of iteration.
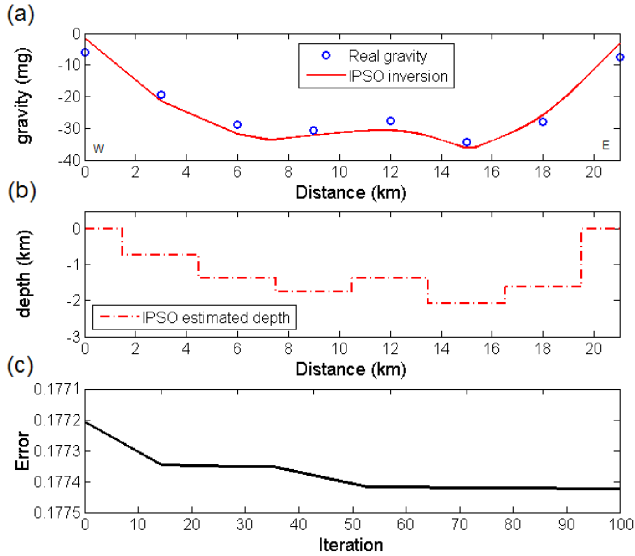
317

Fig. 13. (a) Real gravity along Profile D and computed gravity (b) interpreted basement model by IPSO (c) changes of error estimated by objective function versus the number of iteration.
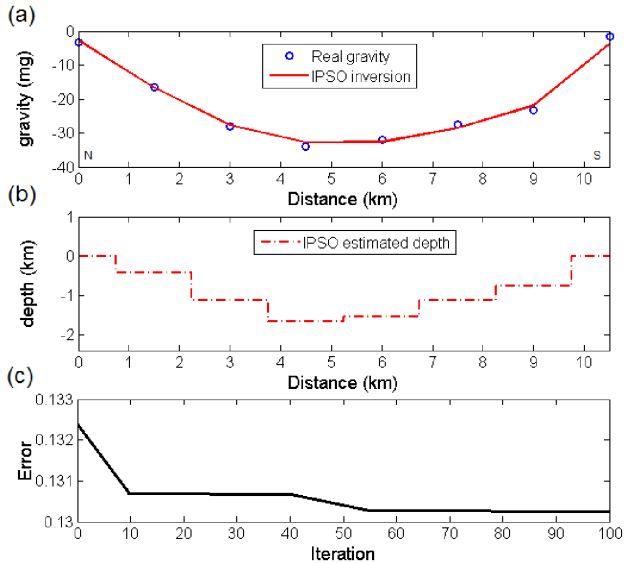

Fig. 14. (a) Real gravity along Profile E and computed gravity (b) interpreted basement model by IPSO (c) changes of error estimated by objective function versus the number of iteration.
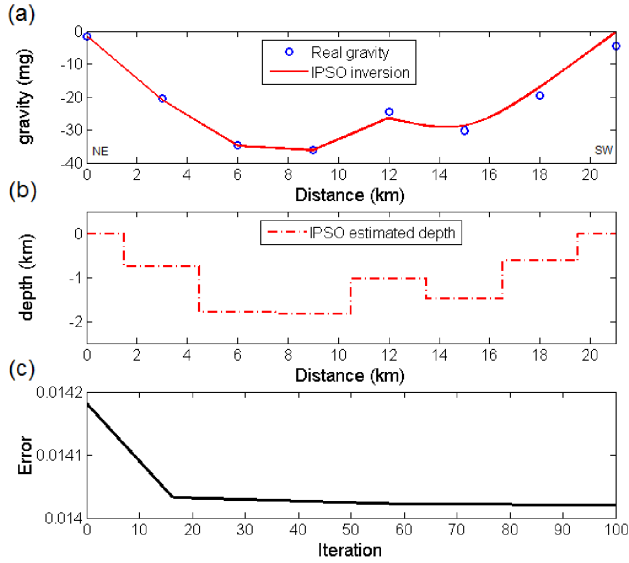
Fig. 15. (a) Real gravity along Profile F and computed gravity (b) interpreted basement model by IPSO (c) changes of error estimated by objective function versus the number of iteration.
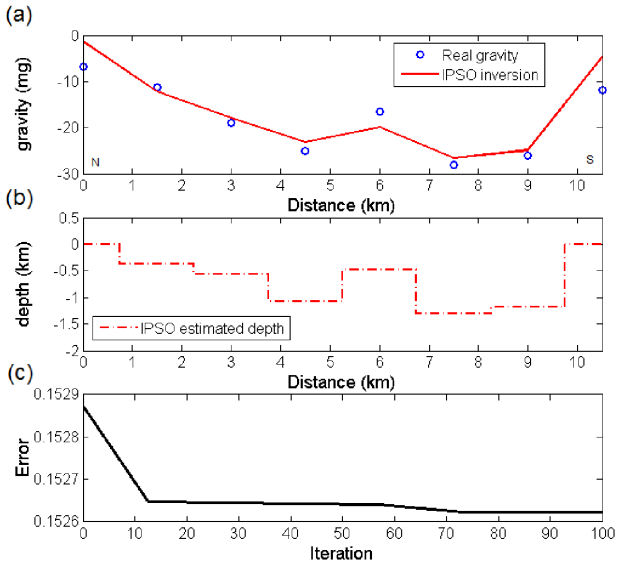

Fig. 16. (a) Real gravity along Profile G and computed gravity (b) interpreted basement model by IPSO (c) changes of error estimated by objective function versus the number of iteration.
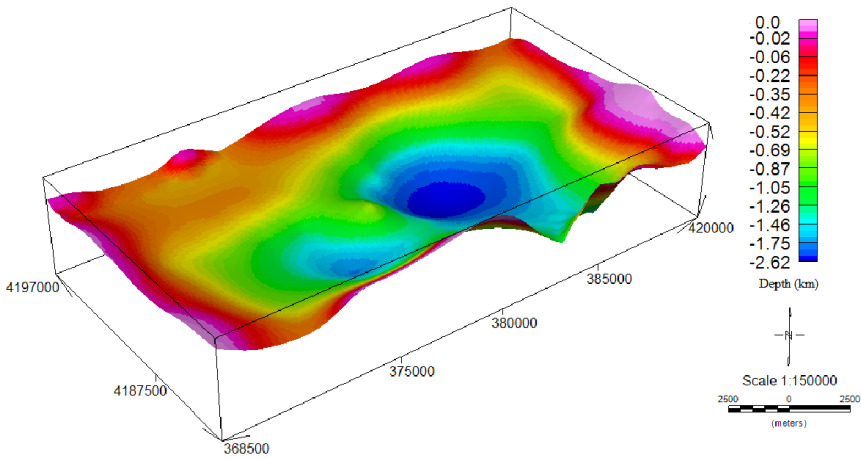
319

Fig. 17. Interpreted 3-D model of the sedimentary basin basement under investigation.

5. Conclusion

In this study, we used the IPSO algorithm for the first time to estimate the thickness of the sedimentary structures and simulate its model using gravity data with and without random noise. The obtained admissible results from the inversion verify the IPSO is an intelligent powerful tool for the inverse modelling of the gravity data. Due to the preset limits on model parameters, the calculated depth and gravity based on synthetic model do not differ too much from the assumed values and are always within the range. The misfit between assumed and calculated gravity was 0.23% in the last iteration.

Also, IPSO was applied to interpret the real gravity data related to a sedimentary basin in Golestan Province, northeastern Iran. We modelled the geometry of the sedimentary basin basement by two-dimensional approach along seven profiles. Furthermore, using the depth values estimated by IPSO from all profiles, the 3-D model of the sedimentary basin basement was generated. The obtained maximum depth value for this sedimentary basin is 2.62 km.

From the comparison between the observed model parameters range (derived using geological data and interpreter experience) with the calculated value of the model parameters and also by analysing the misfit between the observed and calculated gravity in each profile (A, B, C, D, E, F, and

G are 1.314, 1.26, 1.22, 1.88, 1.39, 1.16 and 1.04 percent, respectively) we concluded that the IPSO algorithm is a reliable method to investigate the sedimentary basin depth and make qualified model simulations.

In this research, for the estimation of sedimentary basin depth and simulation of the 3-D shape of sedimentary basin, we used the gravity data along several profiles. Our recommendation for the future investigation of sedimentary basin structures is the direct utilization of the IPSO method; its application can provide the reliable 3-D models and estimates of basin depth using observed gravity data from the gravity network stations.

References

Annecchione M. A., Chouteau M., Keating P., 2001: Gravity interpretation of bedrock topography: the case of the Oak Ridges Moraine, southern Ontario, Canada. J. Appl. Geophys., **47**, 1, 63–81, doi: `10.1016/S0926-9851(01)00047-7`.

Barbosa V. C. F., Silva J. B. C., Medeiros W. E., 1999: Gravity inversion of a discontinuous relief stabilized by weighted smoothness constraints on depth. Geophysics, **64**, 5, 1429–1437, doi: `10.1190/1.1444647`.

Bhattacharyya B. B., Navolio M. E., 1975: Digital convolution for computing gravity and magnetic anomalies due to arbitrary bodies. Geophysics, **40**, 6, 981–992, doi: `10.1190/1.1440592`.

Chakravarthi V., Singh S. B., Ashok Babu G., 2001: INVER2DBASE—A program to compute basement depths of density interfaces above which the density contrast varies with depth. Comput. Geosci., **27**, 10, 1127–1133, doi: `10.1016/S0098-3004(01)00035-8`.

Chakravarthi V., Sundararajan N., 2005: Gravity modeling of $2^{1/2}$-D sedimentary basins — a case of variable density contrast. Comput. Geosci., **31**, 7, 820–827, doi: `10.1016/j.cageo.2005.01.018`.

Chakravarthi V., Sundararajan N., 2006: Gravity anomalies of 2.5-D multiple prismatic structures with variable density: A Marquardt inversion. Pure Appl. Geophys., **163**, 229–242, doi: `10.1007/s00024-005-0008-8`.

Chakravarthi V., Sundararajan N., 2007: Marquardt optimization of gravity anomalies of anticlinal and synclinal structures with prescribed depth-dependent density. Geophys. Prospect., **55**, 4, 571–587, doi: `10.1111/j.1365-2478.2007.00625.x`.

Chakravarthi V., Ramamma B., 2015: Determination of Sedimentary Basin Gravity Inversion using Exponential Density Function Basement Depth: A Space Domain Based: Acta Geophys., **63**, 4, 1066–1079, doi: `10.1515/acgeo-2015-0027`.

Essa K. S., Elhussein M., 2017: 2D dipping dike magnetic data interpretation using a robust particle swarm optimization. Geosci. Instrum. Methods Data Syst. Discuss., **39**, doi: `10.5194/gi-2017-39`.

Essa K. S., Elhussein M., 2018a: Gravity Data Interpretation Using Different New Algorithms: A Comparative Study. In: Zouaghi T.: ravity: Geoscience Applications, Industrial Technology and Quantum Aspect. Licensee InTech., doi: 10.5772/intech open.71086.

Essa K. S., Elhussein M., 2018b: PSO (Particle Swarm Optimization) for Interpretation of Magnetic Anomalies Caused by Simple Geometrical Structures. Pure Appl. Geophys, **175**, 3539–3553, doi: 10.1007/s00024-018-1867-0.

Gadirov V. G., Gadirov K. V., Gamidova A. R., 2016: The deep structure of Yevlakh-Agjabedi depression of Azerbaijan on the gravity-magnetometer investigations. Geodynamics, **20**, 1, 133–143, doi: 10.23939/jgd2016.01.133.

Gallardo-Delgado L. A., Pérez-Flores M. A., Gómez-Treviño E., 2003: A versatile algorithm for joint 3D inversion of gravity and magnetic data. Geophysics, **68**, 3, 949–959, doi: 10.1190/1.1581067.

Karcol R., 2018: The gravitational potential and its derivatives of a right rectangular prism with depth-dependent density following an n-th degree polynomial. Studia Geophys. et Geod., **62**, 427–449, doi: 10.1007/s11200-017-0365-7.

Kennedy J., Eberhart R., 1995: Particle swarm optimization. Proceedings of IEEE Conference on Neural Networks, IEEE Service Center, Piscataway, **4**, 1942–1948, doi: 10.1109/ICNN.1995.488968.

Litinsky V. A., 1989: Concept of effective density: Key to gravity depth determinations for sedimentary basins. Geophysics, **54**, 11, 1474–1482, doi: 10.1190/1.1442611.

Margottini C., Canuti P., Sassa K., 2013: Landslide Science and Practice: Volume 1: Landslide Inventory and Susceptibility and Hazard Zoning. Springer-Verlag, Berlin, Heidelberg, doi: 10.1007/978-3-642-31325-7.

Monteiro Santos F. A., 2010: Inversion of self-potential of idealized bodies' anomalies using particle swarm optimization. Comput. Geosci., **36**, 9, 1185–1190, doi: 10.1016/j.cageo.2010.01.011.

Murthy I. V. R., Krishna P. R., Rao S. J., 1988: A generalized computer program for two-dimensional gravity modeling of bodies with a flat top or a flat bottom or undulating over a mean depth. J. Assoc. Explor. Geophys., **9**, 93–103.

Murthy I. V. R., Rao S. J., 1989: A FORTRAN 77 program for inverting gravity anomalies of two-dimensional basement structures. Comput. Geosci., **15**, 7, 1149–1156, doi: 10.1016/0098-3004(89)90126-X.

Nickabadi A., Ebadzadeh M. M., Safabakhsh R., 2011: A novel particle swarm optimization algorithm with adaptive inertia weight. Appl. Soft Comput., **11**, 4, 3658–3670, doi: 10.1016/j.asoc.2011.01.037.

Pallero J. L. G., Fernández-Martínez J. L., Bonvalot S., Fudym O., 2015: Gravity inversion and uncertainty assessment of basement relief via Particle Swarm Optimization. J. Appl. Geophys., **116**, 180–191, doi: 10.1016/j.jappgeo.2015.03.008.

Pallero J. L. G., Fernández-Martínez J. L., Bonvalot S., Fudym O., 2017: 3D gravity inversion and uncertainty assessment of basement relief via Particle Swarm Optimization. J. Appl. Geophys., **139**, 338–350, doi: 10.1016/j.jappgeo.2017.02.004.

Pallero J. L. G., Fernández-Muñiz M. Z., Cernea A., Álvarez-Machancoses O., Pedruelo-González L. M., Bonvalot S., Fernández-Martínez J. L., 2018: Particle Swarm Optimization and Uncertainty Assessment in Inverse Problems. Entropy, **20**, 2, 96, `doi: 10.3390/e20020096`.

Parsopoulos K. E., Vrahatis M. N., 2002: Recent approaches to global optimization problems through Particle Swarm Optimization. Nat. Comput., **1**, 235–306, `doi: 10.10 23/A:1016568309421`.

Rao C. V., Chakravarthi V., Raju M. L., 1994: Forward modelling: Gravity anomalies of two-dimensional bodies of arbitrary shape with hyperbolic and parabolic density functions. Comput. Geosci., **20**, 5, 873–880, `doi: 10.1016/0098-3004(94)90118-X`.

Rao C. V., Raju M. L., Chakravarthi V., 1995: Gravity modelling of an interface above which the density contrast decreases hyperbolically with depth. J. Appl. Geophys., 34, 1, 63–67, `doi: 10.1016/0926-9851(94)00057-U`.

Roshan R., Singh U. K., 2017: Inversion of residual gravity anomalies using tuned PSO. Geosci. Instrum. Methods Data Syst., **6**, 1, 71–79, `doi: 10.5194/gi-6-71-2017`.

Shi Y., Eberhart R. C., 1998: Parameter selection in particle swarm optimization. In: Porto V. W., Saravanan N., Waagen D., Eiben A. E. (Eds.): Evolutionary Programming VII. EP 1998. Lect. Notes Comput. Sci., **1447**, Springer, Berlin, Heidelberg, 591–600, `doi: 10.1007/BFb0040810`.

Singh K. K., Singh U. K., 2017: Application of particle swarm optimization for gravity inversion of 2.5-D sedimentary basins using variable density contrast. Geosci. Instrum. Methods Data Syst., **6**, 1, 193–198, `doi: 10.5194/gi-6-193-2017`.

Sun J., Li Y., 2014: Adaptive L_p inversion for simultaneous recovery of both blocky and smooth features in a geophysical model. Geophys. J. Int., 197, 2, 882–899, `doi: 10.1093/gji/ggu067`.

Sweilam N. H., El-Metwally K., Abdelazeem M., 2007: Self potential signal inversion to simple polarized bodies using the Particle Swarm Optimization method: A visibility study. J. Appl. Geophys., Egypt. Soc. Appl. Petrophys., **6**, 1, 195–208.

Toushmalani R., 2013a: Comparison result of inversion of gravity data of a fault by particle swarm optimization and Levenberg-Marquardt methods. SpringerPlus, **2**, 462, `doi: 10.1186/2193-1801-2-462`.

Toushmalani R., 2013b: Gravity inversion of a fault by Particle swarm optimization (PSO). SpringerPlus, 2, 315, `doi: 10.1186/2193-1801-2-315`.

Won I. J., Bevis M., 1987: Computing the gravitational and magnetic anomalies due to a polygon: Algorithms and Fortran subroutines. Geophysics, **52**, 2, 232–238, `doi: 10.1190/1.1442298`.

Xin J., Chen G., Hai Y., 2009: A Particle Swarm Optimizer with Multistage Linearly-Decreasing Inertia Weight. International Joint Conference on Computational Sciences and Optimization, 1, 505–508.

Yi L., 2016: Study on an Improved PSO Algorithm and its Application for Solving Function Problem. Int. J. Smart Home, **10**, 3, 51–62, `doi: 10.14257/ijsh.2016.10.3.06`.